CORROSION SCIENCE AND TECHNOLOGY, Vol.22, No.5(2023), pp.314~321 pISSN 1598-6462 / eISSN 2288-6524
[Research Paper] DOI: https://doi.org/10.14773/cst.2023.22.5.314

Evaluation of Inhibition Efficiency of Thymus Extract as a Corrosion Inhibitor of Aluminum Alloy 5083 in an Ethylene Glycol/NaCl Corrosive Medium

H. Hachelef [1], R. Mehdaoui[2,4], K. Hachama[3], M. Amara[4], A. Khelifa[2], A. Benmoussat[2], M. Hadj Meliani[4,†], and Rami K. Suleiman[5,†]

[1]*Materials and Corrosion Equip of LAEPO Research Laboratory Aboubeker Belkaid University of Tlemcen PO Box 230, Tlemcen 13000 Algeria*
[2]*Laboratoire de Génie Chimique (LGC), Faculté des sciences, Université Blida1, B.P.270, Blida 09000, Algeria*
[3]*Laboratoire de Valorisation des Substances Naturelles, Université Djilali Bounaama, Khemis-Miliana, Algeria*
[4]*Laboratoire de Physique Théorique et Matériaux, P.O. Box 151. Hay salem 02000. Université de Chlef, Algeria*
[5]*Interdisciplinary Research Center for Advanced Materials, King Fahd University of Petroleum & Minerals (KFUPM), Dhahran 31261, Saudi Arabia*
(Received November 18, 2022; Revised May 22, 2023; Accepted May 31, 2023)

The aim of the present study was to investigate the effect of thymus extract on corrosion inhibition of aluminum 5083 alloy in a 0.1 M NaCl medium prepared using a mixture of ethylene glycol and water using potentiodynamic and electrochemical impedance spectroscopy (EIS) techniques. The potentiodynamic electrochemical technique showed an increase in corrosion inhibition efficiency starting from 49.63% at a concentration of 0.25 g/L to 92.71% at a maximum concentration of 1.25 g/L of the extract. These results were consistent with those obtained via EIS analysis. Spectral characterization of the tested plant extract using the Fourier-transform infrared spectroscopy (FTIR) technique confirmed the presence of organic compounds having different oxygen and aromatic functionalities in the extract that could help enhance the adsorption of these compounds on the aluminum surface. This study reveals possible adsorption isotherm of the thymus extract on the aluminum surface, supporting a Langmuir isotherm for the adsorption of inhibitor molecules on this surface.

Keywords: *Thymus extract, Inhibition efficiency, Aluminum alloy, Ethylene glycol, Electrochemical impedance*

1. Introduction

Among the various problems caused by corrosion, perforation is a serious issue that can lead to heat transfer fluid leakage. Studies have shown that uninhibited EG degrades to five organic components (glycolic, glyoxylic, formic, carbonic, and oxalic) in the presence of heat, oxygen, and metals, which are commonly found in cooling systems [1,2]. These corrosive elements can chemically attack the aluminum surface within a short period of time (e.g., three weeks) under extreme conditions (212°F) and lead to the formation of oxygen bubbles in an uninhibited solution of EG, the formation of organic components in the fluid, and eventually the clogging of pipes, pumps, valves, etc.

To mitigate or even eliminate these problems, several studies have focused on the anticorrosive protection of alloys using inhibitors that are mainly based on chemicals that can be very toxic and harmful to the environment. The inhibitors added to a corrosive medium can obstruct the active corrosion sites by forming a physically or chemically adsorbed protective layer on the metal surfaces and reducing the corrosion to the safest limits. Plants are proven to be a natural source of organic compounds that can have promising corrosion inhibition properties. The use of plant extracts is considered nowadays a promising and green approach toward the development of effective, biodegradable, and nonpolluting corrosion inhibitors [3–6]. Our group has reported previously the use of thymus Algerian extract as a new eco-friendly corrosion inhibitor for 2024 aluminium alloy in a 1 M HCl medium [7]. This encouraged us to conduct, in this study, an investigation of the inhibition efficiency for the extract of the thymus plant of Algerian origin against the corrosion of aluminum

†Corresponding author: m.hadjmeliani@univ-chlef.dz, ramismob@kfupm.edu.sa

5083 alloy in a corrosive environment composed of a solution of EG and NaCl. An environment containing these two components can highly induce the corrosion of metals, especially in cooling systems. The electrochemical behavior of the metal coupons immersed in a 0.1 M NaCl prepared in EG/water solution in the ratio of (3/7) and with and without the addition of an inhibitor was studied by electrochemical measurement techniques such as the potentiodynamic and electrochemical impedance spectroscopy (EIS) techniques. The effect of the inhibitor concentration as well as the adsorption behavior of the inhibitor molecules were carefully investigated in this study.

2. Materials and methods

2.1 Materials

Aluminum alloy (5083) rectangular coupons of 1 cm^2 dimensions were used as a substrate. The chemical composition of the used alloy was determined using a SPECTROLAB optical-emission spectrophotometer and is shown in Table 1.

The cutting process was chosen in order not to alter the microstructure and corrosion test at the coupon surface, due to its low heat input and the absence of mechanical damage by avoiding the zones to be thermally affected. The pre-treatment of the surface of Al samples was achieved by grinding them with emery paper of 600-1200 grit, rinsing them with bi-distilled water, ultrasonic degreasing in acetone, and finally drying the coupons at room temperature and open to air before use.

2.2 Solution preparation

The extract was prepared by dissolving 5 g of the thymus in 100 mL of EG by a maceration process. Maceration is a batch process that involves soaking the solid in a solvent to extract the soluble components. The EG solvent can increase the permeability of cell walls by facilitating the extraction of a larger number of polar molecules, of medium and low polarity. The maceration under stirring for 24 h and at room temperature allows the depletion of the solvent in extracted compounds and the prevention of their possible alteration or modification by the high temperature.

The corrosion inhibition efficiency of the above-mentioned extract was studied in a 0.1 M NaCl solution prepared in a solvent system composed of EG:water (3:7). The coupons were immersed continuously in a fresh solution of the corrosive medium. The anticorrosion evaluation experiments were conducted in triplicate to ensure reproducibility.

2.3 Electrochemical tests

The electrochemical study was carried out using an Autolab potentiostat brand piloted by Nova 1.7 software, connected to a cell with three-electrode and a double wall thermostat (Tacussel Standard CEC/TH). A saturated calomel electrode (SCE) and platinum electrode have been used as a reference and auxiliary electrode, respectively. The surface area exposed to the electrolyte was masked to be 1 cm^2. The working electrode was immersed in the testing solution for 0.5 h to reach a quasi-stationary value of the open circuit potential prior to the measurements. Tafel polarization curves were obtained by varying the electrode potential from -150 to +150 mV (vs. SCE) at a scan rate of 1 mVs^{-1}. Corrosion current (i_{corr}) and corrosion potential (E_{corr}) were calculated using the Tafel extrapolation treatment employed by the Nova 1.7 software. The electrochemical impedance spectroscopy (EIS) measurements were carried out with the Tacussel electrochemical system that includes a digital potentiostat model Autolab 1.7 system. After obtaining the steady-state current at a corrosion potential, a sine wave voltage (10 mV) peak to peak, at frequencies between 100 kHz and 10 mHz was superimposed on the resting potential. The software automatically controlled the measurements conducted at the rest potentials after 0.5 hours of exposure at 298 K. The impedance diagrams are given in the Nyquist, Bode, and Bode-phase plot representation. Experiments were repeated three times to ensure

Table 1. Chemical composition of the tested aluminum alloy 5083

Eléments	Al	Mn	Si	Mg	Fe	Cu	Co	Zn
Wt%	93.6	0.60	0.139	5.13	0.224	0.142	0.0005	0.036

reproducibility. The corrosion inhibition efficiency (E) derived from the potentiodynamic polarization experiments was calculated based on the value of i_{cor} and using equation 1 below [8]:

$$E(\%) = \frac{(i_{cor}^{0} - i_{cor})}{(i_{cor})} \times 100 \quad (1)$$

Where i_{cor}^{0} and i_{cor} are the corrosion current in the absence and presence of the inhibitor, respectively. The inhibition efficiency that is based on the electrochemical impedance experiments was calculated using equation 2 [4].

$$E(\%) = \frac{(Rt^{0} - Rt)}{Rt^{0}} \times 100 \quad (2)$$

Where Rt and Rt^{0} are the charge transfer resistances of the inhibited and uninhibited solutions, respectively.

The Aluminum specimens were characterized with the aid of an FEI Quanta 650 FEG scanning electron microscope (SEM) (magnification range from 5 to 1,000,000x) (High-vacuum (HV) mode (pressure range 10^{-2}-10^{-4} Pa). The SEM images were taken at the accelerating voltage of 10 kV. Test specimens of 1×1 cm^2 in size were immersed in 100 mL of 0.1 M NaCl solution prepared using an EG:water (3:7) solvent system, and containing a 1.25 g/L of thymus extract for 24 h at 298 K. After washing, the test specimens were dried, and their morphologies were examined.

3. Results

3.1 FTIR analysis of the plant extract

The Fourier-transform infrared spectroscopy (FTIR) spectrum of the solution EG-water (3/7) 0.1 M NaCl containing 1.25 g/L Thymus extract after and before the immersion of the aluminum alloy surface for 24 h was analyzed.

The FTIR analysis was carried out to assess the functional groups present in the thymus extract after immersion. In Fig. 1, we can observe the infrared spectrum. A strong band in the region of 3488–3391 cm^{-1} corresponds to N-H and O-H stretching, as well as the intramolecular hydrogen bonds [9]. The absorption bands at around 2878 and 2939 cm^{-1} can be attributed to C-H symmetric and asymmetric stretching, respectively [10]. There are also absorption bands located at 1650, 1408, and 878 cm^{-1}, which are due to the C=C aromatic stretching vibration, OCO symmetric elongation vibrations, and to C-Cl stretching vibrations, respectively. The spectrum of the plant extract after immersion (Fig. 6b) points out clearly

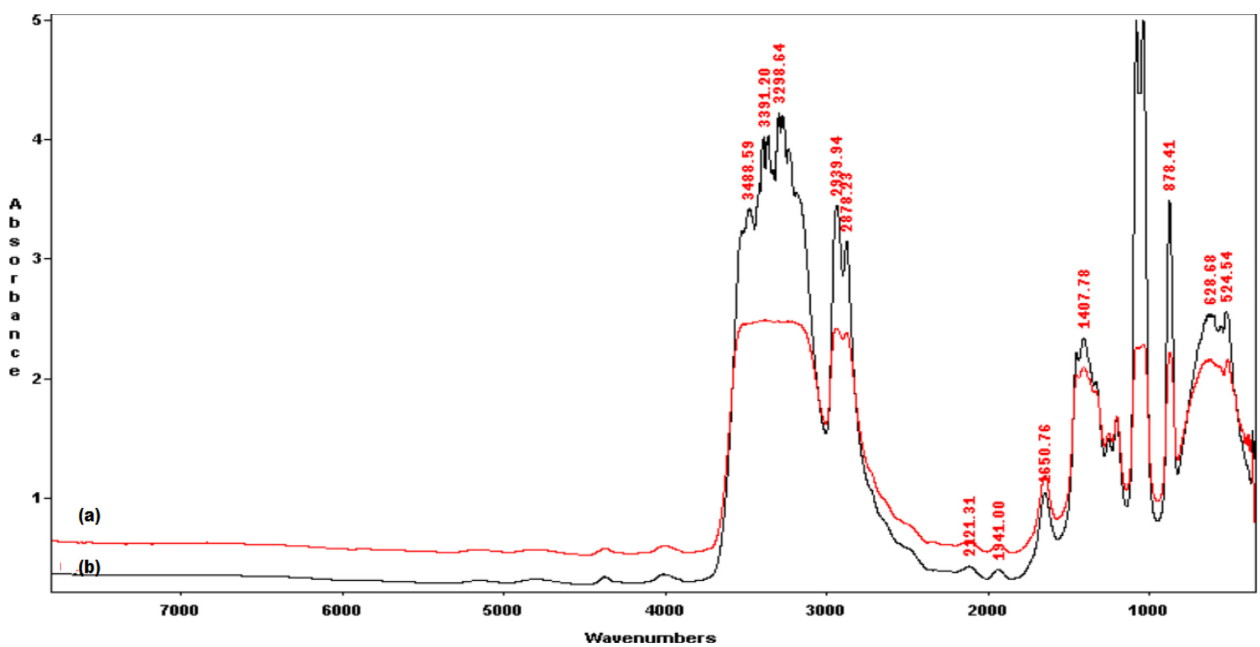

Fig. 1. FTIR Spectrum of the EG-containing 0.1 M NaCl solution and 1.25 g/L thymus extract (a) after and (b) before a 24 h-immersion of the aluminum substrate

the shift in the frequencies at various functional groups indicating the adsorption of these chemical compounds on aluminum alloy surface, from the FTIR and SEM/EDX studies. It can be obviously concluded that the various organic compounds containing OH, O, Cl, ester, and aromatic functionalities are effectively adsorbed on the aluminum surface.

3.2 Effect of inhibitor's concentration

3.2.1 Potentiodynamic polarization

The evaluation of the corrosion inhibition performance of the thymus-plant extract was studied using the potentiodynamic polarization technique. Fig. 2 illustrated the evolution of the corrosion current density versus the potential of aluminum alloy in the EG-containing 0.1 M NaCl solution at different concentrations. The electrochemical parameters including corrosion potential (E_{corr}), corrosion current density (i_{corr}), cathodic Tafel slope (b_c), anodic Tafel slope (b_a), and inhibition efficiency (E%) values were calculated using the Tafel extrapolation method

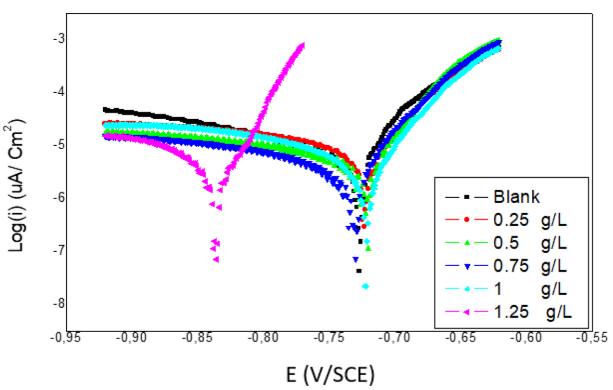

Fig. 2. Potentiodynamic polarization curves for the aluminum alloy samples immersed in an EG-containing 0.1 M NaCl solution at different concentrations of the thymus extract

processed by the Autolab Nova software and presented in Table 2. Based on the results shown in Table 2, a decrease in the current density and corrosion rate which led consequently to an increase in the inhibitory efficiency up to 92.71% was observed when a 1.25 g/L concentration of the inhibitor was used. Additionally, it could be noted that the corrosion potential (E_{corr}) decreased with increasing inhibitor concentration. The reduction in the density of the corrosion current and the corrosion potential is due to the blocking effect of the active sites for corrosion initiation on the metal surface by the adsorbed inhibitors' molecules [11,12].

3.2.2 Electrochemical impedance spectroscopy (EIS)

To attain a better understanding of the mechanism that is taking place at the electrode surface, EIS experiments were undertaken to afford insight into the characteristics and kinetics of the electrochemical processes occurring at the metal/acid interface and how these were modified by the presence of the plant extract molecules.

Fig. 3 depicted the Nyquist, Bode, and Bode-phase plots of the aluminum alloy at different concentrations of thymus extract at 298 k. These diagrams were obtained after 30 min. of immersion in an open circuit. The EIS data of all samples were also simulated using the equivalent circuit shown in Fig. 4 [13] and the obtained fitted electrochemical parameters are listed in Table 3.

The selection of the equivalent circuit for fitting our obtained EIS data was achieved based on the quality of fitting and the physical meaning of the electrochemical system. In this circuit, R_s is the solution resistance, R_p is the charge transfer resistance, and C_{dl} is the double-layer capacitance. This circuit has been reported repeatedly in the literature for fitting EIS data of corrosion systems

Table 2. Potentiodynamic polarization parameters for the corrosion of aluminum alloy in an EG-containing 0.1 M NaCl solution loaded with different concentrations of the thymus-plant extract

Concentration (g/L)	b_a (V/dec)	b_c (V/dec)	E_{corr} (V)	i_{corr} (A/cm²)	(θ)	(E) (%)
Blank	0.93225	0.089771	-0.66302	28.418	-	-
0.25	0.13924	0.037097	-0.68941	14.313	0.49634	49.63403
0.50	0.12238	0.030107	-0.68632	12.236	0.569428	56.94278
0.75	0.071211	0.02781	-0.69626	10.02	0.639806	63.98058
1.00	0.21234	0.034463	-0.69839	7.6966	0.729186	72.91857
1.25	0.067985	0.027017	-0.74302	2.0705	0.927159	92.71588

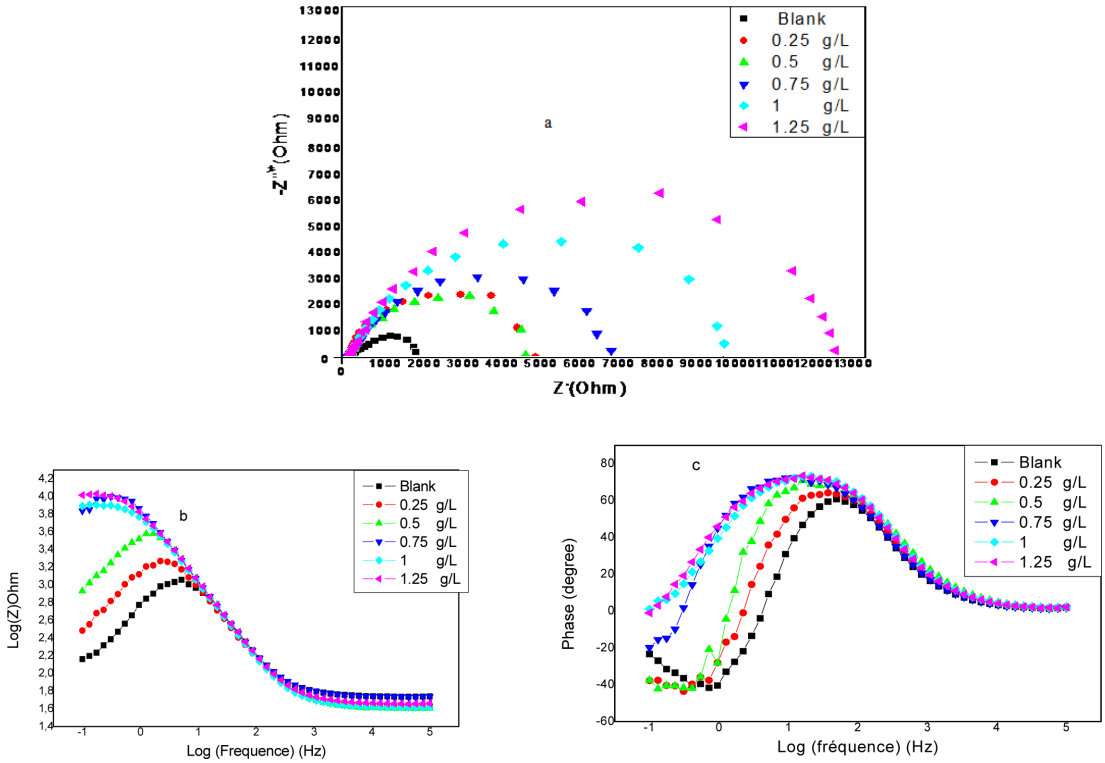

Fig. 3. (a) Nyquist, (b) Bode, and (c) Bode-Phase plots for aluminum alloy immersed in an EG-containing 0.1 M NaCl solution at different concentrations of inhibitor

Table 3. Impedance parameters for aluminum alloy immersed in the 0.1 M NaCl medium for 30 min. in the absence and presence of different concentrations of the inhibitor molecules

Concentration (g/L)	Cdl (μF/Cm^2)	R_p (Ω)	R_s (Ω)	CPE.N	E (%)	(θ)
Blank	108.87	1904.4	50.911	0.99853	-	-
0.50	132.25	4515.4	67.284	1.0003	57.82	0.57824334
1.00	18.75	7598.4	66.122	0.99846	74.93	0.74936829
1.25	1.88×10^{-5}	90891.6	151.49	0.99915	97.90	0.97904757

involving inhibitive pigments [8,13,14]. We found excellent agreement between the experimental and the fitted data obtained using the equivalent circuit shown in Fig. 4. The existence of a one-time constant was confirmed by the presence of a single capacitive loop in the Nyquist spectra of the samples (Fig. 3b) which is linked to the charge transfer process on the aluminum surface.

The fitting parameters shown in Table 3 illustrated an increase in the charge transfer resistance by increasing the inhibitor concentration while the capacity of the double layer decreases as the amount of the extract increases. The decrease in C_d is due to the adsorption of the inhibitor to the metal surface of the aluminum alloy

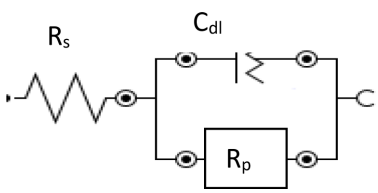

Fig. 4. Equivalent circuit used to fit the EIS data of all aluminum samples exposed to the corrosive saline medium for 30 min. using a 1.25 g/L of the plant extract inhibitor. R_s: solution resistance between the reference electrode and working electrode; R_p: polarization resistance; C_{dl}: double-layer capacitance

which has the effect of reducing the active surface of the electrode. The inhibitor adsorption on the active sites of the steel surface is named for the geometric blocking effect.

The inhibitory efficacy increases with the decrease of the concentration of the inhibitor to reach a maximum value of 97.90% for a concentration equal to 1.25 g/L. This result is in good agreement with those found by potentiodynamic methods.

3.3 Adsorption Isotherm

The mechanism of the adsorption of the inhibitor molecules on the surface of the aluminum coupons during the exposure to the corrosive medium was tested against different isotherms (Langmuir, Frumkin, Temkin, Freundlich, and Flory-Huggins) and only a linear behavior was obtained using the Langmuir isotherm.

This plot depicted in Fig. 5 depicted a clear linearity behavior for the Langmuir isotherm with a correlation coefficient of 0.980. Moreover, the DH_{adsorp} (-16.4 kJ/mol) value extracted from the plot indicated a physisorption mechanism for the inhibitor molecules on the surface of the aluminum substrate [15]. The obtained DH_{adsorp} value in this study is low enough to attribute the adsorption process as due to an electrostatic interaction between the atoms/ions on the metal surface, and the adsorbate molecules mechanism is consistent with physical adsorption.

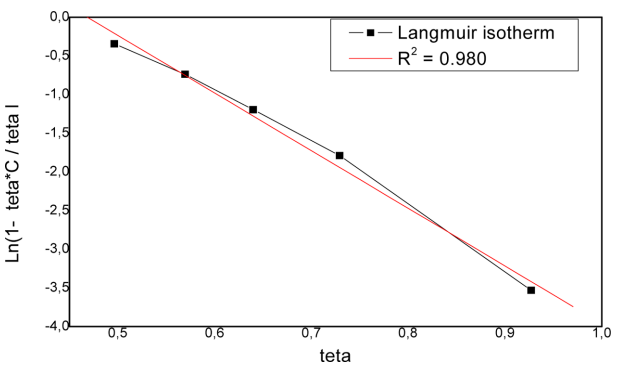

Fig. 5. Langmuir adsorption isotherm for aluminum alloy immersed in an EG-containing 0.1 M NaCl solution at different concentrations of the extract

3.4 Scanning Electron Microscopy (SEM) Analyses

The SEM images of the top surface of the aluminum samples showed the existence of black spots as well as fissures on the aluminum surface in the absence of any inhibitor molecules (Fig. 6a), which can be explained by the deterioration on the aluminum surface caused by the corrosive Cl ions. Opposite to this, an absence of these two phenomena can be observed on the surface of samples

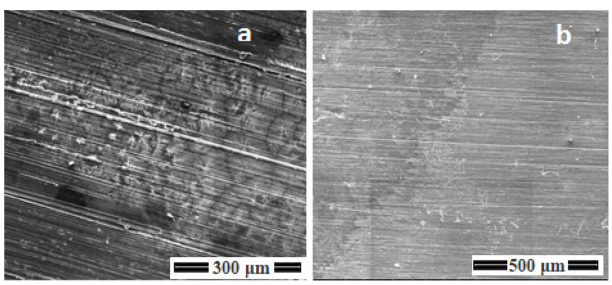

Fig. 6. SEM figures of Al 5083 after 24 hours at 298 k of immersion time in the EG-containing 0.1 M NaCl solution a) without inhibitor and b) with a thymus extract (1.25 g/L)

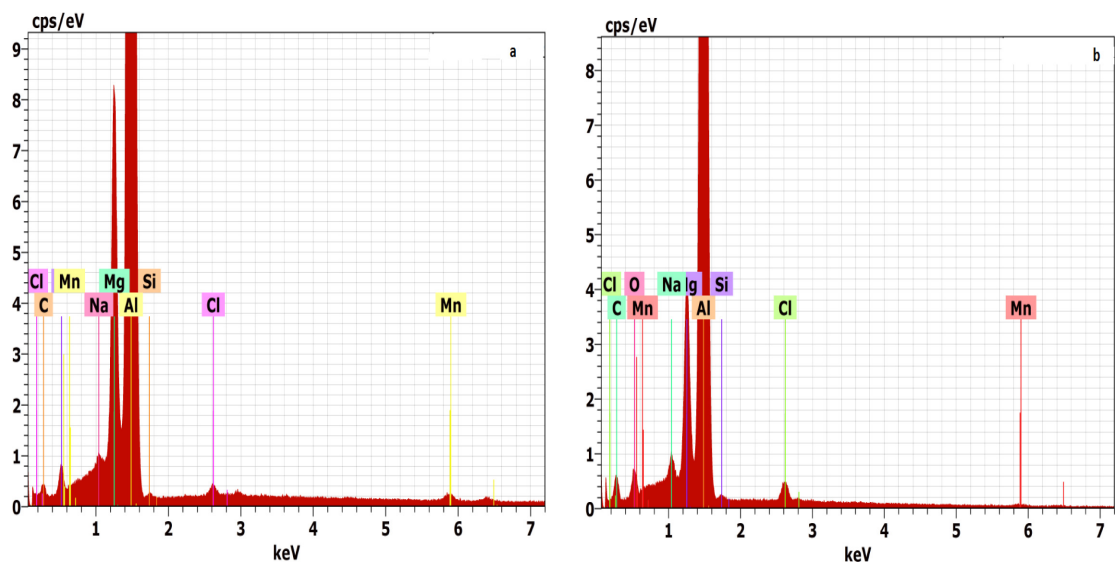

Fig. 7. EDX spectrum of the aluminum alloy surface after immersion time of 24h at 298K in the EG-containing 0.1 M NaCl a) without inhibitor and b) with a thymus extract (1.25 g/L)

immersed in the corrosive medium having the plant extract additive (Fig. 6b). This can be explained by the formation of an adsorbed layer of the thymus extract on the surface of aluminum alloy that helps in preventing the corrosion of the metal surface [16]. The observation of the EDX spectra (Fig. 7) depicted a lower accumulation of the chloride corrosive ions on the aluminum surface immersed in the inhibitor-containing solution (1.25 g/L of the thymus extract) compared to the inhibitor-free sample.

4. Conclusions

In conclusion, the results obtained through this study showed that the thymus-plant extract can be used effectively to inhibit the corrosion of aluminum substrates exposed to glycol-based heat transfer fluid solution and used heavily in the mechanical engine cooling circuits of heavy transport vehicles. The inhibitory efficiency was found to increase as the concentration of extract increased, in which the maximum value was obtained for a concentration of 1.25 g/L of the extract. Moreover, the inhibitory efficiency values obtained via the EIS method were found to be in excellent agreement with those obtained by the potentiodynamic method. The green corrosion-mitigation methodology reported in this study can be a promising alternative to the conventional toxic corrosion inhibitors used to protect aluminum substrates in glycol-containing environments.

References

1. A. N. Ardila-Arias, E. Berrío-Mesa, E. Arriola-Villaseñor, W. F. Álvarez-Gómez, J. A. Hernández-Maldonado, T. A. Zepeda-Partida, L. A. Ortíz-Frade, R. Barrera-Zapata, Degradation of Ethylene Glycol Through Photo-Fenton Heterogeneous System, *Revista Ingenierías Universidad de Medellín*, **18**, 91 (2019). Doi: https://doi.org/10.22395/rium.v18n35a6
2. W. Miller, L. Zhuang, J. Bottema, A. Wittebrood, P. De Smet, A. Haszler, A. Vieregge, Recent development in aluminium alloys for the automotive industry, *Materials Science and Engineering A*, **280**, 37 (2000). Doi: https://doi.org/10.1016/S0921-5093(99)00653-X
3. S. A. Umoren, M. M. Solomon, I. B. Obot, R. K. Sulei man, A critical review on the recent studies on plant biomaterials as corrosion inhibitors for industrial metals, *Journal of Industrial and Engineering Chemistry*, **76**, 91 (2019). Doi: https://doi.org/10.1016/j.jiec.2019.03.057
4. S. A. Umoren, M. M. Solomon, I. B. Obot, R. K. Suleiman, Date palm leaves extract as a green and sustainable corrosion inhibitor for low carbon steel in 15 wt.% HCl solution: the role of extraction solvent on inhibition effect, *Environmental Science and Pollution Research*, **28**, 40879 (2021). Doi: https://doi.org/10.1007/s11356-021-13567-5
5. M. A. Benghalia, C. Fares, A. Khadraoui, M. H. Meliani, R. K. Suleiman, A. A. Sorour, I. M. Dmytrakh, Z. Azari, Assessment of corrosion inhibitory effect of ruta chalepensis flavonoid extracts on API 5L X52 steel in 1M HCL Medium, *Environmental Engineering and Management Journal*, **18**, 2009 (2019). Doi: https://doi.org/10.30638/eemj.2019.191
6. N. A. Odewunmi, S. A. Umoren, Z. M. Gasem, S. A. Ganiyu, Q. Muhammad, l-Citrulline: An active corrosion inhibitor component of watermelon rind extract for mild steel in HCl medium, *Journal of the Taiwan Institute of Chemical Engineers*, **51**, 177 (2015). Doi: https://doi.org/10.1016/j.jtice.2015.01.012
7. A. Khadraoui, A. Khelifa, K. Hachama, R. Mehdaoui, Thymus algeriensis extract as a new eco-friendly corrosion inhibitor for 2024 aluminium alloy in 1M HCl medium, *Journal of Molecular Liquids*, **214**, 293 (2016). Doi: https://doi.org/10.1016/j.molliq.2015.12.064
8. I. B. Obot, S. A. Umoren, Z. M. Gasem, R. Suleiman, B. El Ali, Theoretical prediction and electrochemical evaluation of vinylimidazole and allylimidazole as corrosion inhibitors for mild steel in 1M HCl, *Journal of Industrial and Engineering Chemistry*, **21**, 1328 (2015). Doi: https://doi.org/10.1016/j.jiec.2014.05.049
9. A. M. Barberena-Fernández, P. M. Carmona-Quiroga, M. T. Blanco-Varela, Interaction of TEOS with cementitious materials: Chemical and physical effects, *Cement and Concrete Composites*, **55**, 145 (2015). Doi: https://doi.org/10.1016/j.cemconcomp.2014.09.010
10. R. K. Suleiman, A. Y. Adesina, A. M. Kumar, M. M. Rahman, F. A. Al-Badour, B. El Ali, Anticorrosion Properties of a Novel Hybrid Sol–Gel Coating on Aluminum 3003 Alloy, *Polymers (Basel)*, **14**, 1798 (2022). Doi: https://doi.org/10.3390/polym14091798
11. A. Farhadian, A. Rahimi, N. Safaei, A. Shaabani, M. Abdouss, A. Alavi, A theoretical and experimental study of castor oil-based inhibitor for corrosion inhibition of mild steel in acidic medium at elevated temperatures,

Corrosion Science, **175**, 108871 (2020). Doi: https://doi.org/10.1016/j.corsci.2020.108871

12. F. M. Mahgoub, A. M. Hefnawy, E. H. Abd Alrazzaq, Corrosion inhibition of mild steel in acidic solution by leaves and stem extract of Acacia nilotica, *Desalination and WATER Treatment*, **169**, 49 (2019). Doi: https://doi.org/10.5004/dwt.2019.24681
13. A. Kouache, A. Khelifa, H. Boutoumi, S. Moulay, A. Feghoul, B. Idir, S. Aoudj, Experimental and theoretical studies of Inula viscosa extract as a novel eco-friendly corrosion inhibitor for carbon steel in 1 M HCl, *Journal of Adhesion Science and Technology*, **36**, 988 (2022). Doi: https://doi.org/10.1080/01694243.2021.1956215
14. Q. Ma, S. Qi, X. He, Y. Tang, G. Lu, 1,2,3-Triazole derivatives as corrosion inhibitors for mild steel in acidic medium: Experimental and computational chemistry studies, *Corrosion Science*, **129**, 91 (2017). Doi: https://doi.org/10.1016/j.corsci.2017.09.025
15. D. Wang, B. Xiang, Y. Liang, S. Song, C. Liu, Corrosion control of copper in 3.5wt.% NaCl Solution by Domperidone: Experimental and Theoretical Study, *Corrosion Science*, **85**, 77 (2014). Doi: https://doi.org/10.1016/j.corsci.2014.04.002
16. A. Sedik, D. Lerari, A. Salci, S. Athmani, K. Bachari, İ.H. Gecibesler, R. Solmaz, Dardagan Fruit extract as eco-friendly corrosion inhibitor for mild steel in 1 M HCl: Electrochemical and surface morphological studies, *Journal of the Taiwan Institute of Chemical Engineers*, **107**, 189 (2020). Doi: https://doi.org/10.1016/j.jtice.2019.12.006